Drift, partial drift and Darwin's proposition

I. Eames, S. E. Belcher and J. C. R. Hunt

Drift, partial drift and Darwin's proposition

By I. EAMES[1], S. E. BELCHER[1]† AND J. C. R. HUNT[2]

[1] Department of Applied Mathematics and Theoretical Physics, University of Cambridge,
Silver Street, Cambridge CB3 9EW, UK

[2] Meteorological Office, Bracknell, Berks RG12 2SZ, UK

A body moves at uniform speed in an unbounded inviscid fluid. Initially, the body is infinitely far upstream of an infinite plane of marked fluid; later, the body moves through and distorts the plane and, finally, the body is infinitely far downstream of the marked plane. Darwin (1953) suggested that the volume between the initial and final positions of the surface of marked fluid (the drift volume) is equal to the volume of fluid associated with the 'added-mass' of the body.

We re-examine Darwin's (1953) concept of drift and, as an illustration, we study flow around a sphere. Two lengthscales are introduced: ρ_{max}, the radius of a circular plane of marked particles; and x_0, the initial separation of the sphere and plane. Numerical solutions and asymptotic expansions are derived for the horizontal Lagrangian displacement of fluid elements. These calculations show that depending on its initial position, the Lagrangian displacement of a fluid element can be either positive – a Lagrangian drift – or negative – a Lagrangian reflux. By contrast, previous investigators have found only a positive horizontal Lagrangian displacement, because they only considered the case of infinite x_0. For finite x_0, the volume between the initial and final positions of the plane of marked fluid is defined to be the 'partial drift volume', which is calculated using a combination of the numerical solutions and the asymptotic expansions. Our analysis shows that in the limit corresponding to Darwin's study, namely that both x_0 and ρ_{max} become infinite, the partial drift volume is not well-defined: the ordering of the limit processes is important. This explains the difficulties Darwin and others noted in trying to prove his proposition as a mathematical theorem and indicates practical, as well as theoretical, criteria that must be satisfied for Darwin's result to hold.

We generalize our results for a sphere by re-considering the general expressions for Lagrangian displacement and partial drift volume. It is shown that there are two contributions to the partial drift volume. The first contribution arises from a reflux of fluid and is related to the momentum of the flow; this part is spread over a large area. It is well-known that evaluating the momentum of an unbounded fluid is problematic since the integrals do not converge; it is this first term which prevented Darwin from proving his proposition as a theorem. The second contribution to the partial drift volume is related to the kinetic energy of the flow caused by the body: this part is Darwin's concept of drift and is localized near the centreline. Expressions for partial drift volume are generalized for flow around arbitrary-shaped two- and three-dimensional bodies. The partial drift volume is shown to depend on the solid angles the body subtends with the initial and final positions of the plane of marked fluid. This result explains why the proof of Darwin's proposition depends on the ratio ρ_{max}/x_0.

† Present address: Department of Meteorology, University of Reading, Reading, RG6 2AU, UK

An example of drift due to a sphere travelling at the centre of a square channel is used to illustrate the differences between drift in bounded and unbounded flows.

1. Introduction

When a sphere moves in an unbounded inviscid fluid, one might intuitively expect, as Darwin (1953) remarked, that there would be a net flux of fluid in the opposite direction to the motion of the sphere; a reflux of fluid. Detailed calculations by Darwin (1953) show that there is a volume of fluid that drifts in the same direction as the sphere. This flux of fluid drifting with the sphere can be interpreted as a 'potential-flow wake' behind the body.

Darwin (1953) examined the motion of an arbitrarily shaped solid body in an unbounded region of inviscid fluid. The body starts infinitely far from an infinite plane of marked fluid, and travels at a constant speed towards the plane, which is then distorted by the passage of the body. Darwin defined the *drift volume* to be the volume between the initial and final positions of the surface of marked fluid and suggested that drift volume is equal to the volume of fluid associated with the hydrodynamic mass of the body (figure 1). The hydrodynamic mass of a body is the mass of fluid that must be added to the body when calculating the total kinetic energy; it is commonly referred to as 'added mass' (Batchelor 1967, p. 407). Darwin's proposition is an appealing result and has been further investigated by Lighthill (1956), Yih (1985) and Benjamin (1986).

Darwin's proposition has been referred to several times as Darwin's theorem. But it has been pointed out by Darwin himself and by Benjamin (1986) that the drift volume depends critically on the method of evaluation of certain integrals and so the proposition cannot be proved to be a mathematical theorem without delicate qualifications. We therefore prefer the term 'Darwin's proposition'.

Darwin's proposition has been used to interpret measurements of bubble motion and other two-phase flows. For example, Bataille, Lance & Marie (1991) set up an experiment with a lower layer of fluid that was dyed and slightly denser than an upper layer of fluid. Bubbles were released beneath the interface, which was distorted by the passage of a bubble. The volume of fluid that drifted with a bubble was measured and found to be equal to Darwin's calculation, i.e. half the bubble volume which is equal to the added mass volume of the bubble for potential flow. Interestingly, Rivero's (1990) numerical calculations of the added-mass volume of accelerating rigid spheres and bubbles in viscous flows ($Re \approx 100$) also agree with the volume calculated using potential flow.

In this paper, Darwin's proposition is investigated and generalized by considering the deformation of a finite-sized plane of marked fluid that is initially placed a finite distance from the body. When the body is subsequently infinitely far from its initial position, the volume between the final and initial plane of marked fluid elements is defined here to be the *partial drift volume* (figure 2a). To illustrate the properties of partial drift volume, we consider flow around a sphere and examine in detail the Lagrangian displacement of a circular plane of marked fluid, of radius ρ_{max}, that starts a distance x_0 from the sphere. In §2, trajectories of fluid particles are calculated numerically and using asymptotic analysis, which extends the earlier results of Lighthill (1956). The partial drift volume is calculated in §3, for various values of x_0 and ρ_{max}, using a combination of the asymptotic formulae and numerical results.
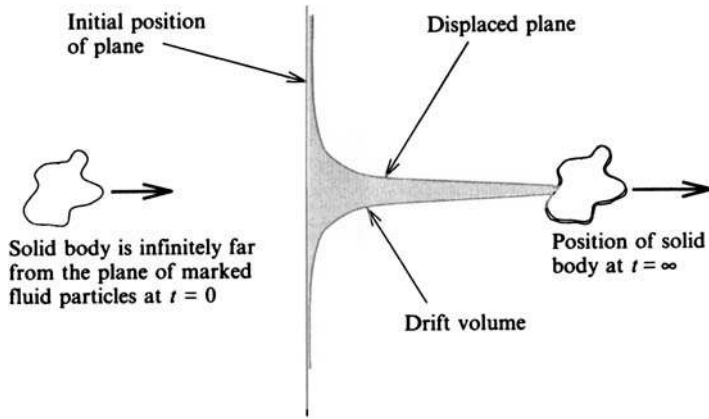
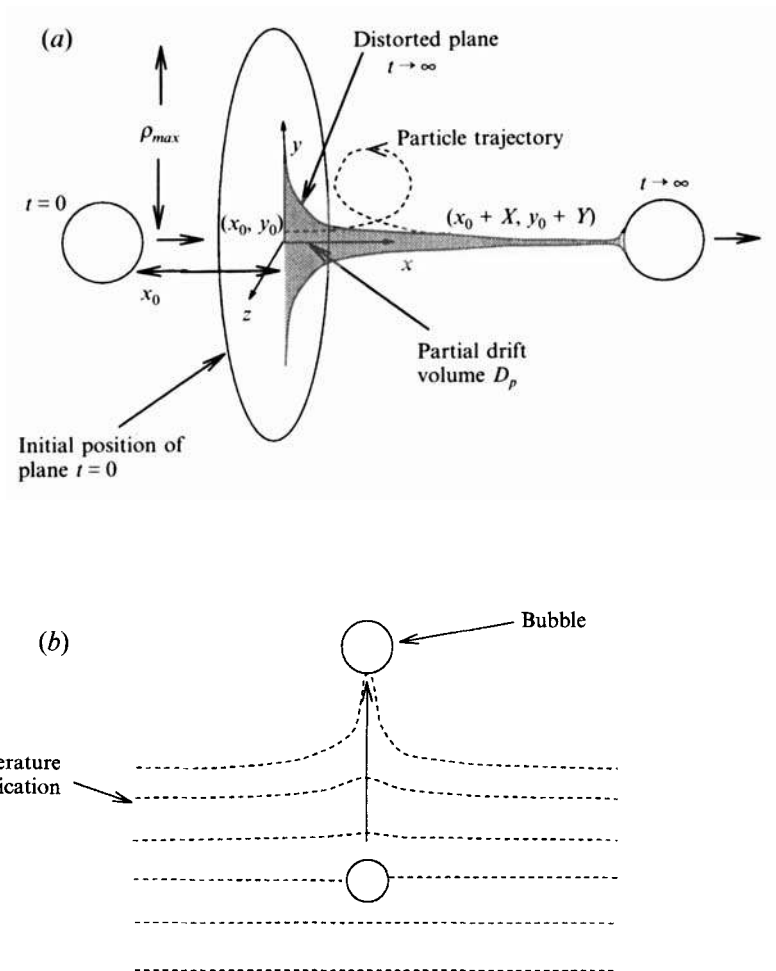FIGURE 1. Sketch of the drift volume (as defined by Darwin).

FIGURE 2. Definition sketch of the partial drift volume. (*a*) Notation, (*b*) to show a typical problem.
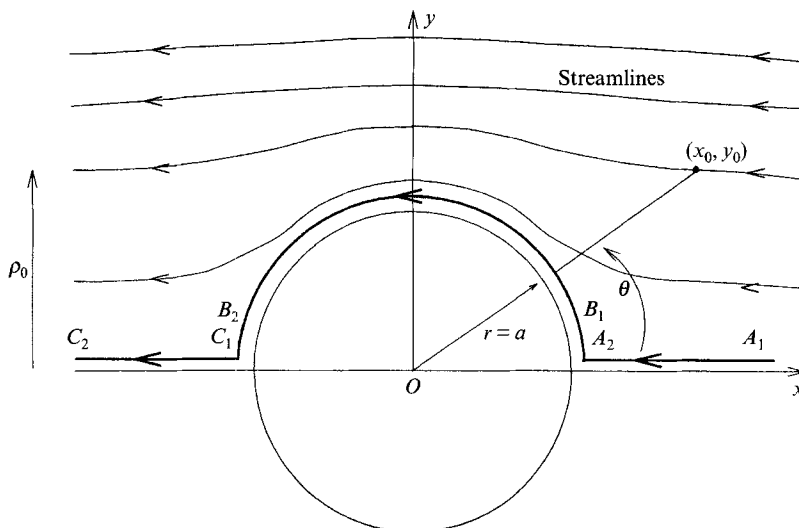
FIGURE 3. Streamlines close to the sphere.

It is shown that, in the configuration studied by Darwin (1953), Yih (1985) and Benjamin (1986) when both x_0 and ρ_{max} are infinite, the problem is not well-posed, because the drift volume is not well-defined. Yih's procedure does in effect assume as $\rho_{max}/x_0 \rightarrow 0$ as $x_0 \rightarrow \infty$.

In §4 a general expression for horizontal Lagrangian displacement is derived for an arbitary potential fluid flow superimposed on a constant-mean-velocity flow. The partial drift volume is shown to depend on the solid angles subtended by the body and initial and final positions of the plane of marked fluid. This analysis is generalized to arbitrarily shaped two- and three-dimensional bodies.

In §5, we use our results for drift due to a sphere in unbounded flow to indicate how drift in bounded flow can be calculated. The sphere is assumed to travel along the centreline of a square tube. This three-dimensional example can be applied to practical problems (e.g. the experiments of Bataille *et al.* 1991; Kowe *et al.* 1988).

Finally it is worth noting that there are an increasing number of practical fluid mechanics problems whose solution depends on having a good estimate of the drift volume (e.g. Kowe *et al.* 1988). For example, the partial drift volume is also of importance when large particles are ejected into a cloud of smaller particles, or a rising bubble formed in a temperature gradient (figure 2*b*).

2. Horizontal Lagrangian displacement for flow around a sphere

Consider the inviscid flow caused by a fixed sphere of radius a in a uniform stream of speed $-U\boldsymbol{x}$, where U is constant and $\boldsymbol{x}$ is the unit vector parallel to the x-axis. The flow is axisymmetric and so it is sufficient to consider a single (x, y) plane, shown in figure 3. In spherical polar coordinates the velocity potential and streamfunction are

$$\phi = -U \left(r + \frac{a^3}{2r^2} \right) \cos \theta, \quad \psi = -U \left(\frac{r^2}{2} - \frac{a^3}{2r} \right) \sin^2 \theta, \quad (2.1a, b)$$

where r is the distance from the origin and θ is the angle made with the x-axis. The velocity components are

$$u_r = \frac{\mathrm{d}r}{\mathrm{d}t} = -U\left[1 - \frac{a^3}{r^3}\right]\cos\theta, \quad u_\theta = \frac{\mathrm{d}\theta}{\mathrm{d}t} = U\frac{\sin\theta}{r^4}\left[r^3 + \frac{a^3}{2}\right]. \qquad (2.2a, b)$$

Lighthill's (1956) notation is used, so that a fluid element marked at time $t = 0$ with Cartesian coordinates (x_0, y_0) is advected to the position $(-\infty, \rho_0)$ as $t \to \infty$. Equation (2.1b) is used to relate ρ_0, x_0 and y_0, so that

$$\rho_0 = y_0\left(1 - \frac{a^3}{(x_0^2 + y_0^2)^{3/2}}\right)^{1/2}. \qquad (2.3)$$

It is more convenient to expresss the position of a marked fluid element at time t in terms of polar coordinates $(r(t), \theta(t))$, which is related to its ultimate position by

$$r^3 - \frac{\rho_0^2 r}{\sin^2\theta} - a^3 = 0. \qquad (2.4)$$

The roots of the cubic equation (2.4) can be found analytically (e.g. Abramowitz & Stegun 1965, p. 17), and when $\sin\theta > (4/27)^{1/6}\rho_0/a$

$$r = \left[\frac{a^3}{2} + \left(-\frac{\rho_0^6}{27\sin^6\theta} + \frac{a^6}{4}\right)^{1/2}\right]^{1/3} + \left[\frac{a^3}{2} - \left(-\frac{\rho_0^6}{27\sin^6\theta} + \frac{a^6}{4}\right)^{1/2}\right]^{1/3}, \qquad (2.5)$$

whereas when $\sin\theta < (4/27)^{1/6}\rho_0/a$

$$r = \frac{2\rho_0}{\sqrt{3}\sin\theta}\cos\alpha, \quad \text{where} \quad \cos 3\alpha = \frac{3^{3/2}a^3}{2\rho_0^3}\sin^3\theta. \qquad (2.6)$$

The horizontal Lagrangian displacement of the fluid elements, X, is defined to be

$$X = \int_0^\infty (U + u_x)\mathrm{d}t = \int_0^\infty U\frac{a^3(2\cos^2\theta - \sin^2\theta)}{2r^3}\mathrm{d}t. \qquad (2.7)$$

This expression is manipulated using (2.2b) to eliminate $\mathrm{d}t$ and (2.4) to remove the r^3 term; X is then given by

$$X(\rho_0, x_0) = \int_{\theta_0}^\pi \frac{a^3(2 - 3\sin^2\theta)r\sin\theta}{3a^3\sin^2\theta + 2\rho_0^2 r}\mathrm{d}\theta, \qquad (2.8)$$

where $\theta_0 = \arctan(y_0/x_0)$. The horizontal Lagrangian displacement is written in (2.8) as a function of ρ_0, the final vertical position of the marked fluid element, and θ_0 the initial horizontal position. This choice of variables simplifies the calculation of the partial drift volume in §4. The integral (2.8) cannot be expressed in closed form and approximations are found using asymptotic analysis. Also, the dependence of $X(\rho_0, x_0)$ on ρ_0 is found directly from expression (2.8) rather than using, as Lighthill (1956) did, $X = \lim_{t\to\infty}(Ut + x)$.

2.1. *Asymptotic formulae for $X(\rho_0, x_0)$ far from the centreline*

Marked fluid elements whose final positions are far from the symmetry axis have $\rho_0/a \gg 1$, and the root of the cubic equation (2.4) can be approximated by

$$r = \frac{\rho_0}{\sin\theta}\left[1 + \frac{1}{2}\frac{a^3}{\rho_0^3}\sin^3\theta - \frac{3}{8}\frac{a^6}{\rho_0^6}\sin^6\theta + O\left(\frac{a^9}{\rho_0^9}\right)\right], \qquad (2.9)$$

$$X \approx \frac{9a^6\pi}{64y_0^5}$$

$$X \approx \frac{4a}{3}\log\left(\frac{2a3^{3/4}}{y_0}\right)$$

$$X \approx -\frac{a^3|x_0|}{y_0^3}$$

$$X \approx -\frac{a^3}{2x_0^2}$$

$$X = 0$$

$$X \approx \frac{9a^6\pi}{64y_0^5}$$

$$X \approx \frac{4a}{3}\log\left(\frac{2a3^{3/4}}{y_0}\right)$$
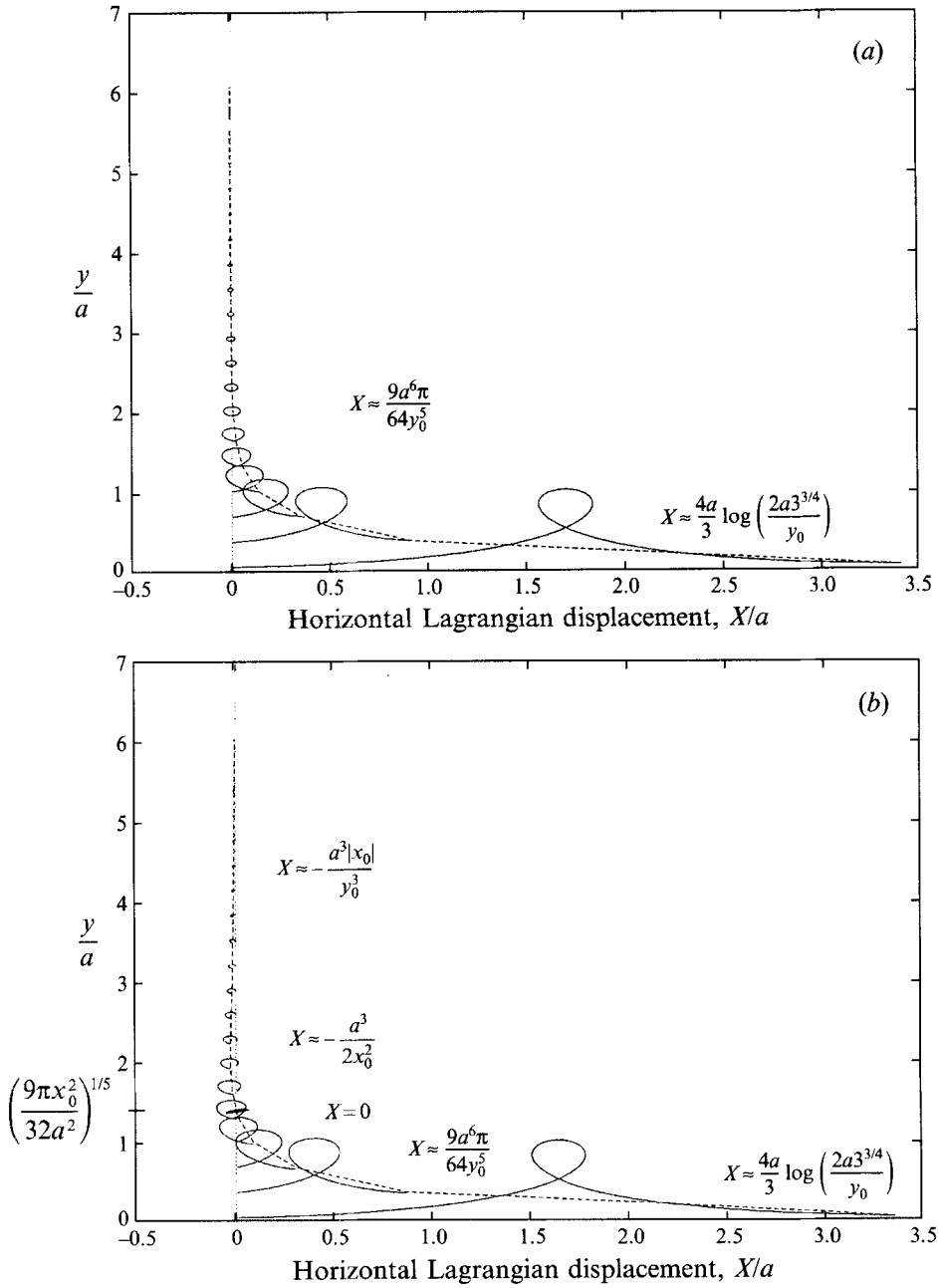
$$\left(\frac{9\pi x_0^2}{32a^2}\right)^{1/5}$$

FIGURE 4 (*a*, *b*). For caption see facing page.

which is equation (64) in Lighthill (1956). In this approximation, the integral in (2.8) can be evaluated and the horizontal Lagrangian displacement is

$$X = \frac{a^3}{2\rho_0^2}\left[\cos^3\theta_0 - \cos\theta_0\right]$$

$$-\frac{3a^6}{4\rho_0^5}\left[\frac{3\theta_0}{16} - \frac{1}{64}\sin 6\theta_0 + \frac{5}{64}\sin 4\theta_0 - \frac{13}{64}\sin 2\theta_0 - \frac{3\pi}{16}\right] + O\left(\frac{a^9}{\rho_0^8}\right), \quad (2.10)$$
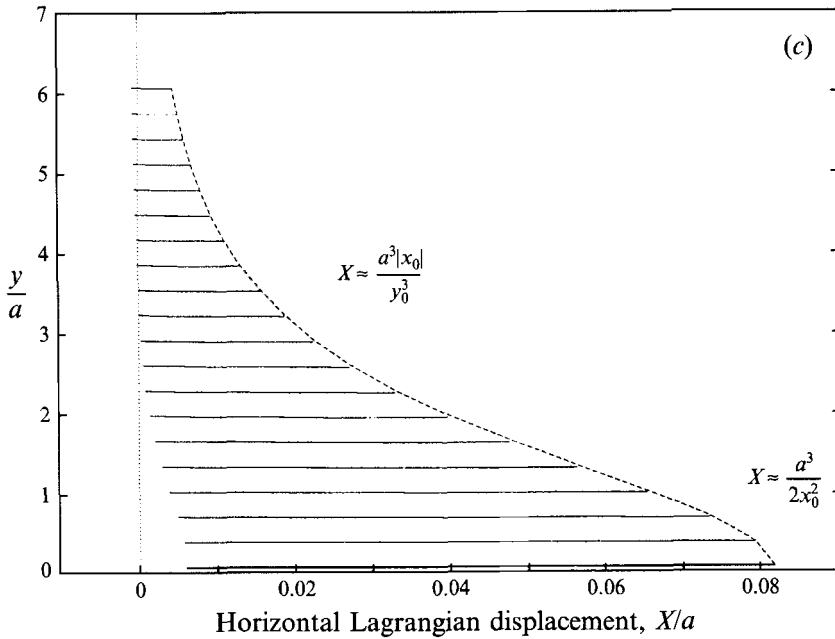
FIGURE 4. Plot of the trajectories of marked fluid particles on planes (*a*) $x_0 = 50.0a$, (*b*) $x_0 = 2.5a$, (*c*) $x_0 = -2.5a$.

which expresses the displacement in terms of the initial position, through the θ_0 dependence, and the final position, through the ρ_0 dependence. Far from the centreline, $y_0 \gg a$ so that from (2.3), $\rho_0 \approx y_0$ and $\theta_0 \approx \arctan(\rho_0/x_0)$.

We further approximate (2.10) in order to calculate the horizontal Lagrangian displacement of fluid elements marked far in front of the sphere, when $\theta_0 \to 0$, and far behind the sphere, when $\theta_0 \to \pi$. When $\theta_0 \to 0$ and $\rho_0/a \gg 1$, (2.10) gives

$$X(\rho_0, x_0) = \frac{9a^6\pi}{64\rho_0^5} - \frac{a^3}{2x_0^2} + O\left(\frac{a^2\rho_0^2}{x_0^4}\right). \tag{2.11}$$

Lighthill (1956) obtained the first term of (2.11) (his equation (67)) when he considered the limit of $x_0 \to \infty$. The new second term arises from x_0 being finite and gives an important contribution to X. When $\theta_0 \to \pi$ and $\rho_0/a \gg 1$, (2.10) gives

$$X(\rho_0, x_0) = \frac{a^3}{2x_0^2} + \frac{3a^6}{20x_0^5} + O\left(\frac{a^3\rho_0^2}{x_0^4}\right), \tag{2.12}$$

which is independent of ρ_0 and therefore flat.

The horizontal Lagrangian displacement of a fluid element marked far from the symmetry axis and with x_0 small is now calculated by allowing $\theta_0 \to \pi/2$ in (2.10); this shows that

$$X(\rho_0, x_0) = -\frac{a^3 x_0}{2\rho_0^3} + \frac{a^3 x_0^3}{2\rho_0^5} + O\left(\frac{a^6}{\rho_0^5}\right). \tag{2.13}$$

The asymptotic expansions show that there is a surface of marked fluid particles in the region $x_0 > 0$, $y_0 > 0$, $\rho_0 \gg a$, on which the horizontal displacement is zero. From
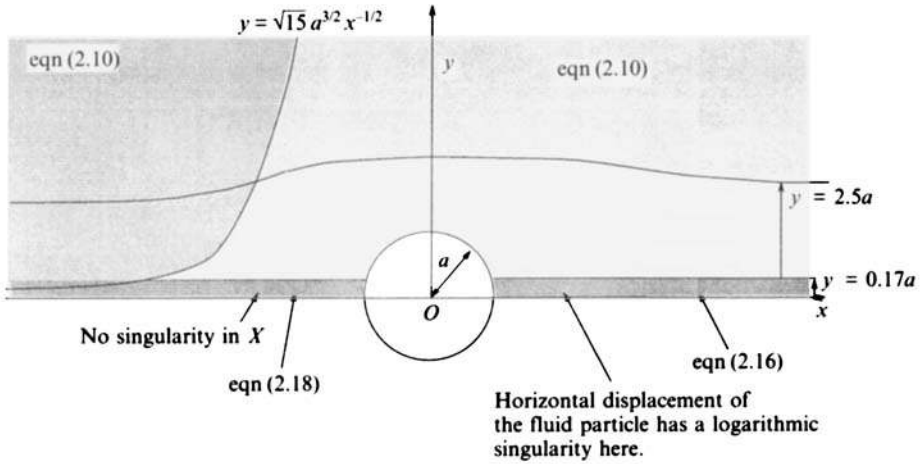
FIGURE 5. Schematic of where the errors of the asymptotic expansions are small.

(2.11) this surface is given approximately by

$$y_0 \sim \left(\frac{9\pi a^3 x_0^2}{32}\right)^{1/5}. \tag{2.14}$$

Finite x_0 were not analysed by Darwin (1953) or Lighthill (1956): they considered the limit $x_0 \to \infty$. Consequently, they found positive horizontal Lagrangian displacement for all y_0 (see figure 4a). Equation (2.13) shows that if x_0 is positive and finite then, far from the centreline, fluid elements are displaced in the direction opposite to the motion of the sphere. This region of negative horizontal displacement, i.e. a region of reflux, is a consequence of introducing a finite x_0 and has interesting implications for practical purposes. An example of a region of reflux is shown in figure 4(b).

The asymptotic formula (2.10) is used in §3 to evaluate the partial drift volume so it is important to find where this is a good approximation to X. A suitable restriction, obtained from (2.8), is $3a^3 \sin^2 \theta < \frac{1}{10} 2\rho_0^2 r$. The most restrictive inequality for $x_0 < 0$ is

$$\frac{3a^3}{2y_0^2(1 - [a^3/(x_0^2 + y_0^2)^{3/2}])(x_0^2 + y_0^2)^{1/2}} \leqslant \frac{1}{10}. \tag{2.15}$$

When $|x_0| \gg y_0$, this implies $y_0 > \sqrt{15}a^{3/2}/x_0^{1/2}$ and when $|x_0| \ll y_0$ it requires $y_0 > 2^{4/3}a$. These conditions define two regions that are sketched in figure 5. If $x_0 > 0$, the smallest value of r is r_{min} and occurs when $\theta = \pi/2$, where

$$r_{min} \left(1 - a^3/r_{min}^3\right)^{1/2} = \rho_0.$$

A suitable requirement for (2.10) to be a good approximation to X for $x_0 > 0$ is $3a^3 < \frac{1}{10} 2\rho_0^2 r_{min}$ from which we obtain the requirement $\rho_0 > 16^{1/3}(15/16)^{1/2}a \approx 2.5a$.

Lighthill (1956) estimated that the region of convergence for the expansion of X, when $\rho_0 \gg a$ and $x_0 \to \infty$, is $\rho_0 > 1.5a$. We find that when $\rho_0 > 2.5a$ the first two terms of the asymptotic expansion (2.11) approximate $X(\rho_0, x_0)$ with relative error 5%.

2.2. *Asymptotic expansions of* $X(\rho_0, x_0)$ *close to the centreline*

Lighthill (1956) derived two expressions for X close to the centreline when $x_0 \to \infty$: one along the streamline segment A_1A_2 and another along B_1B_2 (see figure 3). These expressions were matched to determine the horizontal Lagrangian displacement. We use a similar approach to calculate X when $x_0 > a$ and $\rho_0/a \ll 1$, but generalize Lighthill's (1956) analytical results by analysing finite x_0.

If $R = (x_0^2 + y_0^2)^{1/2}$, we find a horizontal Lagrangian displacement given by

$$
X(\rho_0, x_0) = \frac{4a}{3} \left(1 + \frac{\rho_0^2}{3a^2}\right) \ln\left(\frac{2a3^{3/4}}{\rho_0}\right) - \frac{\pi a}{3\sqrt{3}} \left(1 - \frac{\rho_0^2}{3a^2}\right) - 2a - \frac{\rho_0^2}{9a}
$$

$$
+ \frac{a}{3}\left(1 + \frac{\rho_0^2}{3a^2}\right) \ln\left(\frac{R - a}{(R^2 + aR + a^2)^{1/2}}\right) + \frac{a}{\sqrt{3}}\left(1 - \frac{\rho_0^2}{3a^2}\right) \arctan\left(\frac{\sqrt{3}a}{2R + a}\right)
$$

$$
+ \frac{\rho_0^2 R^2}{3(R^3 - a^3)} + O\left(\frac{\rho_0^4}{a^3}\right),
\tag{2.16}
$$

which reduces to Lighthill's equation (73) when $R \to \infty$, namely,

$$
X(\rho_0) = \frac{4a}{3} \left(1 + \frac{\rho_0^2}{3a^2}\right) \ln\left(\frac{2a3^{3/4}}{\rho_0}\right) - \frac{\pi a}{3\sqrt{3}} \left(1 - \frac{\rho_0^2}{3a^2}\right) - 2a - \frac{\rho_0^2}{9a}.
\tag{2.17}
$$

When $x_0 < -a$, a similar calculation shows that the horizontal Lagrangian displacement is

$$
X(\rho_0, x_0) = -\frac{a}{3}\left(1 + \frac{\rho_0^2}{3a^2}\right) \ln\left(\frac{R - a}{(R^2 + aR + a^2)^{1/2}}\right) - \frac{a}{\sqrt{3}}\left(1 - \frac{\rho_0^2}{3a^2}\right) \arctan\left(\frac{\sqrt{3}a}{2R + a}\right)
$$

$$
- \frac{\rho_0^2 R^2}{3(R^3 - a^3)} + O\left(\frac{\rho_0^4}{a^3}\right).
\tag{2.18}
$$

The expansions (2.18) and (2.12) are both appropriate and are the same when $R \gg a$ and $x_0 \ll -a$. The region of overlap is sketched in figure 6.

Lighthill (1956) found that the region of convergence of the expansion (2.18) is $\rho_0 < 0.4a$. We find that the horizontal Lagrangian displacement (2.17) can be represented by the first two terms of its asymptotic expansion when $\rho_0 < a\sqrt{3}/10 \approx 0.17a$.

2.3. *Numerical calculation of fluid particle trajectories*

The asymptotic expansions derived in the previous sections were supplemented with numerical calculations to obtain solutions for horizontal Lagrangian displacement over the whole ranges of x_0 and ρ_0. Trajectories in the Cartesian coordinate system were obtained by solving

$$
\frac{dx}{dt} = \frac{\partial \phi}{\partial x}, \quad \frac{dy}{dt} = \frac{\partial \phi}{\partial y},
$$

subject to the initial condition $x = x_0$ and $y = y_0$ at time $t = 0$.

Figure 4 shows examples of fluid particle trajectories plotted in Cartesian coordinates as $(X(\rho_0, x_0, t), y(\rho_0, x_0, t))$, together with the deformed marked planes, for $x_0 = 50.0a, 2.5a, -2.5a$. The horizontal Lagrangian displacement close to the centreline when $x_0 = 50.0a$ is approximately the same as when $x_0 \to \infty$. If $x_0 \to \infty$ (figure 4a), the horizontal Lagrangian displacement is positive for all y_0 so that all the marked fluid elements drift with the sphere. But, if x_0 is large and positive, as in $x_0 = 2.5a$ (figure 4b), there is a region of reflux (negative X).
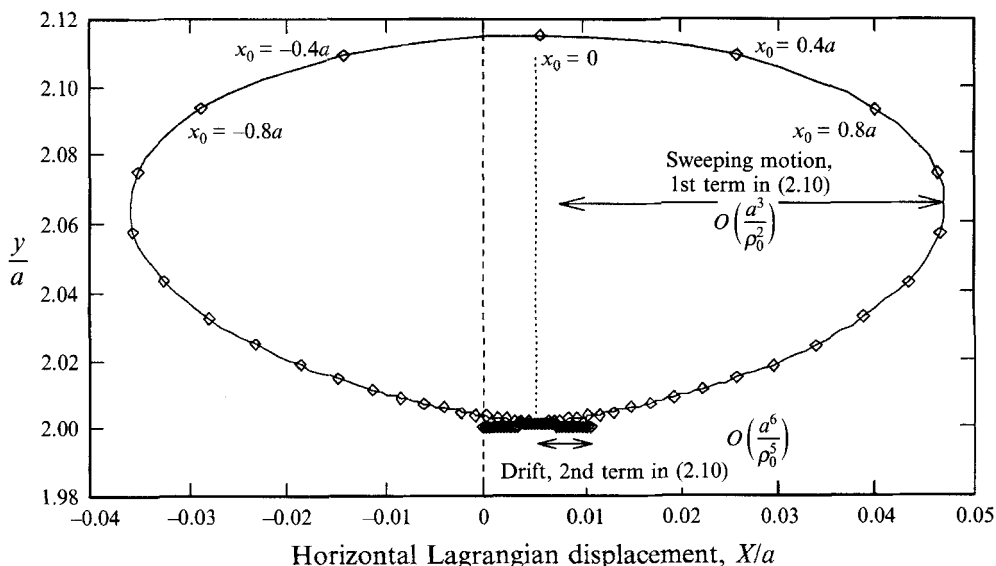
FIGURE 6. Trajectory of a single marked fluid element on the streamline $\rho_0 = 2.0a$. The diamonds
($\diamond$) indicate where marked fluid particles start on the streamline.

When $x_0 \rightarrow -\infty$, the perturbation to the fluid flow due to the presence of the sphere is neglible so that the Lagrangian displacement of the marked fluid particles is zero. The fluid particles drift in the same direction as the sphere when x_0 is large and negative as shown in figure 4c, which uses $x_0 = -2.5a$.

The trajectories plotted in figure 4 show two distinct features: a sweeping motion and a drift. Close to the centreline the contribution to X from the positive drift is larger than from the sweeping motion, but far from the centreline the sweeping motion is larger than the drift forwards. Figure 6 shows that the sweeping motion gives a larger contribution than the small drift forwards and that the displacement of the fluid particle depends on where it is initially marked. In §4 we explain how the sweeping motion and the drift give two separate contributions to partial drift volume.

3. Partial drift volume

The drift volume is defined to be the volume between the initial and final position of the marked plane, i.e. the integral of the drift, X, over the marked plane (Darwin 1953). By analogy, we define the *partial drift volume*, D_p, to be the volume between the final and initial positions of a marked plane of finite extent which is initially placed a finite distance from a solid body (see figure 2a). For a circular marked plane that is distorted by a sphere, the partial drift volume is

$$D_p(\rho_{max}, x_0) = \int_0^{\rho_{max}} X(\rho_0, x_0) 2\pi\rho_0 d\rho_0, \tag{3.1}$$

where ρ_{max} is the radius of the marked circle after a large time, when the sphere has moved infinitely far away. Partial drift volume therefore generalizes the definition of drift volume by introducing two parameters, namely ρ_{max} and x_0. We shall show that the variation of D_p with ρ_{max} and x_0 has important implications for the usefulness of Darwin's proposition in practical applications and explains the difficulties in proving Darwin's proposition as a mathematical theorem.

We define D to be the drift volume calculated using Darwin's method, so that D is the volume of fluid associated with the hydrodynamic mass of the body.

3.1. *Asymptotic expression for D_p when the marked plane starts far from the sphere*

The asymptotic expressions derived in §2 for the drift are now used to find approximations to the partial drift volume. Two limits are treated: firstly, the marked plane starts far upstream of the sphere and, secondly, the plane starts far downstream of the sphere.

Darwin (1953, §2) showed that when $x_0 \to \infty$ and $\rho_{max}/x_0 \to 0$ the drift volume is equal to the volume of fluid associated with the hydrodynamic mass of the solid body, e.g. for a sphere $D = \frac{2}{3}\pi a^3$. When $x_0 \to \infty$ and ρ_{max} is large but finite, the partial drift volume, D_p, is close to D.

If $x_0 \to \infty$ then the partial drift volume, D_p, is related to drift volume, D, by

$$D = D_p + \int_{\rho_{max}}^{\infty} X 2\pi\rho_0 \, d\rho_0. \tag{3.2}$$

If $\rho_{max}/a \gg 1$, and $\rho_{max} \ll x_0$, then the integral can be evaluated because X can be approximated by (2.11). The result is that

$$D_p(\rho_{max}, x_0) \sim \frac{2}{3}\pi a^3 - \frac{3\pi^2 a^6}{32\rho_{max}^3} \quad \text{as } x_0 \to \infty. \tag{3.3}$$

It is clear from this asymptotic analysis that, when $x_0 \to \infty$ and ρ_{max} is finite, D_p is only approximately equal to D. Benjamin (1986) however suggested that, under these conditions, D_p is equal to D. Benjamin's (1986) error can be traced to the manipulation given in going from his equation (5) to (6).

A second limit is that the marked plane starts far downstream of the sphere, i.e. $x_0 \ll -a$. The approximate expression for X given in (2.12) is then valid over the whole range of ρ_0 and the partial drift volume can be evaluated; it is

$$D_p(\rho_{max}, x_0) \sim 2\pi \int_0^{\rho_{max}} \frac{a^3}{2x_0^2}\rho_0 \, d\rho_0 = \frac{\pi\rho_{max}^2 a^3}{2x_0^2} \quad \text{as } x_0 \to -\infty. \tag{3.4}$$

This result is surprising because it shows that D_p can remain finite if x_0 and ρ_{max} both become infinite, i.e. no matter how far the plane starts behind the sphere, if ρ_{max} is sufficiently large, the drift volume can have any value. This observation indicates why Darwin's proposition must be qualified before it can be stated as a theorem.

3.2. *Asymptotic expansions for D_p when the marked plane is large*

If $x_0 \ll -a$ then (2.10) is a good approximation to X over all ρ_0 and the partial drift volume can be evaluated:

$$D_p(\rho_{max}, x_0) \sim \pi a^3 - \frac{\pi a^3}{(1 + (\rho_{max}/x_0)^2)^{1/2}} \quad \text{as } \rho_{max} \to \infty. \tag{3.5}$$

When $x_0 \gg a$ and $\rho_0/a \gg 1$, (2.10) is approximately equal to

$$X(\rho_0, x_0) \sim \lim_{x_0 \to \infty} X(\rho_0, x_0) + \frac{a^3}{2\rho_0^2}[\cos^3\theta_0 - \cos\theta_0]. \tag{3.6}$$

Equation (2.16) is approximately

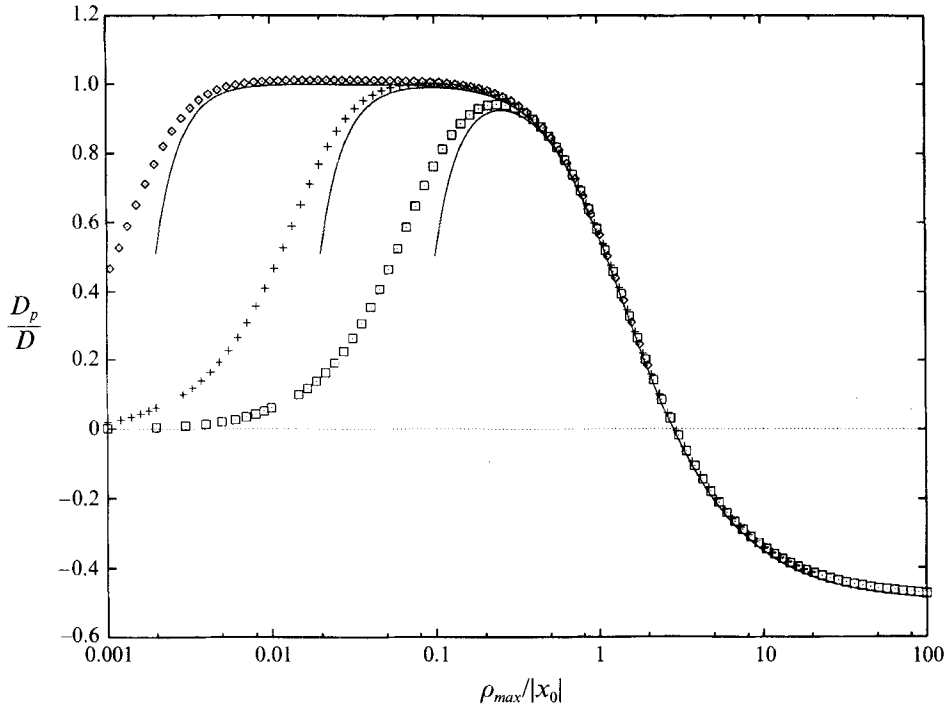$$X(\rho_0, x_0) \sim \lim_{x_0 \to \infty} X(\rho_0, x_0) - \frac{a^3}{2x_0^2}, \tag{3.7}$$

FIGURE 7. Normalized partial drift volume (D_p/D) plotted against $\rho_{max}/|x_0|$ for: $\diamond$, $x_0 = 500.0a$; $+$, $x_0 = 50.0a$; and $\Box$, $x_0 = 10.0a$. Equation (3.9) is plotted as _____.

when $\rho_0/a \ll 1$. The second terms of the right-hand sides of (3.6) and (3.7) are due to introducing finite x_0, and they asymptotically match when $x_0 \to \infty$. This leads to the suggestion that

$$D_p \sim \lim_{x_0 \to \infty} D_p - \pi a^3 + \frac{\pi a^3}{(1 + (\rho_{max}/x_0)^2)^{1/2}}. \tag{3.8}$$

Using (3.3), we find that

$$D_p \sim -\frac{\pi a^3}{3} - \frac{3\pi^2 a^6}{32\rho_{max}^3} + \frac{\pi a^3}{(1 + (\rho_{max}/x_0)^2)^{1/2}}. \tag{3.9}$$

Below, we find a good agreement of (3.9) with the numerically calculated value of D_p for a large range of ρ_{max}/x_0.

3.2.1. *Numerical calculation of partial drift volume*

Long computational times are required to follow the large numbers of marked fluid particles needed to evaluate D_p and so we used the asymptotic expansions of $X(\rho_0, x_0)$ where they are good approximations. Consequently, when $x_0 > a$, $X(\rho_0, x_0)$ was calculated numerically only in the range $0.1 \leqslant \rho_0/a \leqslant 4.0$. Equation (2.10) was used to approximate X when $\rho_0/a > 4.0$ and (2.16) when $\rho_0/a < 0.1$. When $x_0 < -a$, the horizontal Lagrangian displacement is evaluated using (2.10) for $\rho_0/a > 4.0$ and numerically when $\rho_0/a < 4.0$.

Figures 7 and 8 show values of $D_p(\rho_{max}, x_0)$ normalized by Darwins drift $D = \frac{2}{3}\pi a^3$. In figure 7 partial drift volume is plotted against $\rho_{max}/|x_0|$ for various fixed values of x_0 larger than a, whereas in figure 8, x_0 is less than $-a$. Figure 7 shows that if
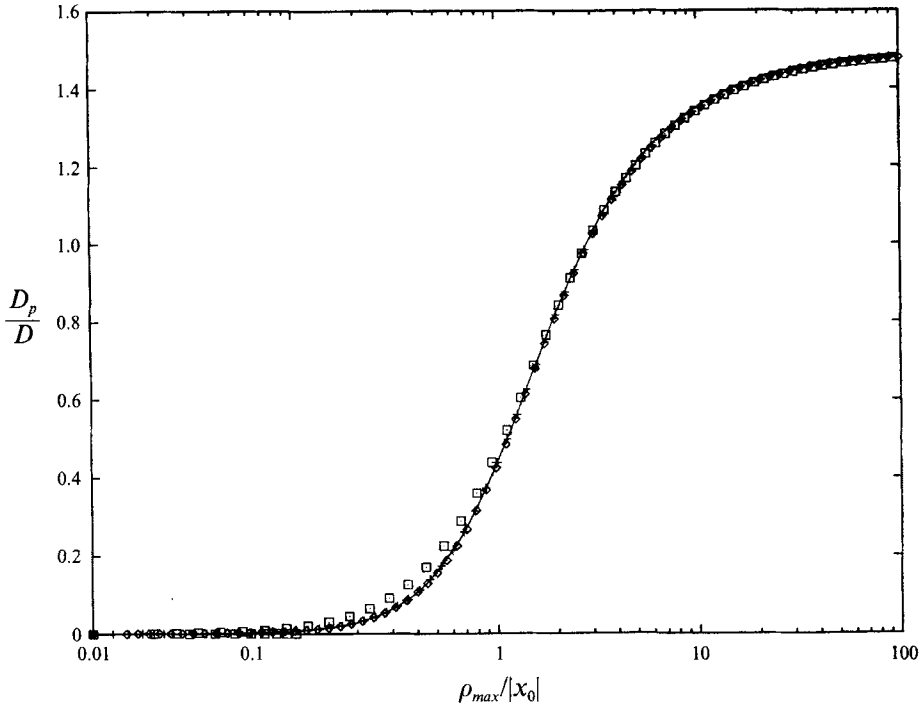
FIGURE 8. Normalized partial drift volume (D_p/D) plotted against $\rho_{max}/|x_0|$ for: $\diamond$, $x_0 = -10.0a$; $+$, $x_0 = -4.0a$; and $\square$, $x_0 = -1.0a$. Equation (3.5) is plotted as ____.

$\rho_{max}/x_0 \ll 1$, $D_p/D \rightarrow 1$; by contrast when $\rho_{max}/x_0 \gg 1$, $D_p/D \rightarrow -\frac{1}{2}$. The asymptotic expressions for $D_p(\rho_{max}, x_0)$ are also plotted for comparision.

The curves in figures 7 and 8 show that when x_0 becomes large, D_p/D asymptotes to a function of ρ_{max}/x_0. When both x_0 and ρ_{max} become infinite (the case studied by Darwin 1953 and Benjamin 1986) our calculations show clearly that the value of D_p/D depends on how the double limit is approached. First taking $x_0 \rightarrow \pm\infty$ and then $\rho_{max} \rightarrow \infty$ is equivalent to

$$\lim_{\rho_{max}\rightarrow\infty}\lim_{x_0\rightarrow\pm\infty} D_p(\rho_{max}, x_0) = \lim_{\rho_{max}/x_0\rightarrow\pm 0} D_p(\rho_{max}, x_0),$$

whereas first taking $\rho_0 \rightarrow \infty$ and then $x_0 \rightarrow \pm\infty$ implies

$$\lim_{x_0\rightarrow\pm\infty}\lim_{\rho_{max}\rightarrow\infty} D_p(\rho_{max}, x_0) = \lim_{\rho_{max}/x_0\rightarrow\pm\infty} D_p(\rho_{max}, x_0).$$

Figures 7 and 8 show that the partial drift volume asymptotes to different values in these two limits. Hence the drift volumes as calculated by Darwin (1953) and Benjamin (1986) require careful definitions and therefore cautious use in experiments! We are able to state Darwin's result as a theorem: when a solid body passes through a *large* marked plane that is initially *infinitely* far in front of the body (i.e. $\rho_{max}/x_0 \rightarrow 0$), then the volume between the initial and final position of the marked plane is the volume of fluid associated with the hydrodynamic mass of the body. Mathematically, this theorem can be stated concisely as

$$\lim_{\rho_{max}/x_0\rightarrow 0} D_p(\rho_{max}, x_0) = D.$$

4. General analysis

Our detailed analysis of drift and partial drift volume for flow around a sphere shows several interesting features which we now generalize to bodies of arbitrary shape.

4.1. General expression for the horizontal Lagrangian displacement

In §2 it was shown that horizontal Lagrangian displacement can be positive – a drift – or negative – a reflux. A general analysis is now developed to explore the processes that cause the displacement.

For potential flow around an arbitrarily shaped body fixed in a uniform stream of speed $-Ux$, the horizontal Lagrangian displacement is

$$X = \int (U + u_x)\mathrm{d}t = -\int \frac{1}{U}(u_x U + v^2)\mathrm{d}t + \int \frac{1}{U}q^2\mathrm{d}t, \qquad (4.1)$$

where $q = \{(U + u_x)^2 + u_y^2 + u_z^2\}^{1/2}$, the fluid particle speed is $v = (u_x^2 + u_y^2 + u_z^2)^{1/2}$ and u_x, u_y, u_z are the velocity components of the fluid relative to the body. Two results from potential flow theory, namely (Yih 1985)

$$\frac{\mathrm{d}\phi}{\mathrm{d}t} = v^2, \qquad \left(\frac{\partial x}{\partial \phi}\right)_{\psi,\chi} = \frac{u_x}{v^2}, \qquad (4.2a,b)$$

are needed to manipulate (4.1) into

$$X = -\int_{\phi_0}^{\phi_1} \frac{1}{U}\left(U\left(\frac{\partial x}{\partial \phi}\right)_{\psi,\chi} + 1\right)\mathrm{d}\phi + \int_0^t \frac{1}{U}q^2\mathrm{d}t. \qquad (4.3)$$

The first integral can be evaluated; it is

$$\int_{\phi_0}^{\phi_1} \frac{1}{U}\left\{U\left(\frac{\partial x}{\partial \phi}\right)_{\psi,\chi} + 1\right\}\mathrm{d}\phi = \left[\frac{\phi}{U} + x\right]_{\phi_0}^{\phi_1}$$

$$= \int_{x_0}^{x_1(t)} \frac{1}{U}(U + u_x)\mathrm{d}x + \int_{y_0}^{y_1(t)} \frac{1}{U}u_y\mathrm{d}y + \int_{z_0}^{z_1(t)} \frac{1}{U}u_z\mathrm{d}z. \qquad (4.4)$$

Hence $X(x_0, y_0, z_0, t)$ is given by

$$X(x_0, y_0, z_0, t) = -\int_{x_0}^{x_1(t)} \frac{1}{U}(U + u_x)\mathrm{d}x - \int_{y_0}^{y_1(t)} \frac{1}{U}u_y\mathrm{d}y - \int_{z_0}^{z_1(t)} \frac{1}{U}u_z\mathrm{d}z + \int_0^t \frac{1}{U}q^2\mathrm{d}t.$$
$$(4.5)$$

Here $x_1(t) = x_0 - Ut + X(x_0, y_0, t)$, $y_1(t)$ and $z_1(t)$ are the Cartesian coordinates of the fluid element at time t.

Assuming in the far field that the flow due to the solid body can be approximated by a dipole of strength $\frac{1}{2}Ua^3$, then far from the centreline (so that $y_0 \gg x_0 \gg a$) the first term in (4.5) is $O(Ua^3/r^2)$ and dominates the other terms, which are $O(Ua^6/r^5)$. The horizontal Lagrangian displacement is therefore given approximately by

$$X(x_0, y_0, z_0, t) \sim -\frac{1}{U}\int_{x_0}^{x_1(t)}(U + u_x)\mathrm{d}x, \qquad (4.6)$$

which is the momentum defect between two points along a streamline. Equation (4.6) represents the sweeping motion seen in figure 6 and is approximately equal to the first term in (2.10).

If a fluid particle starts close to the centreline, so that $y_0 \ll a$ and $x_0 \gg y_0$, the first term in (4.5) is $O(Ua^3/r^2)$, as in the previous paragraph. Such particles travel close to the stagnation points on the body, where they have high residence time. Hence these particles will be displaced a large distance forward. Therefore the last term in (4.5) dominates and the horizontal Lagrangian displacement is approximately

$$X(x_0, y_0, z_0, t) \sim \frac{1}{U} \int_0^t q^2 \mathrm{d}t, \tag{4.7}$$

which is the total kinetic energy along a streamline per unit area normal to the direction of motion of the sphere. Expression (4.7) represents the drift of marked fluid with the body and is approximately equal to the second term in (2.10).

4.2. *Interpretation of* D_p

The horizontal Lagrangian displacement given by (4.4) and (4.5) is now used to evaluate the partial drift volume. The fluid flow due to the motion of a sphere is equivalent to the flow due to a dipole. Furthermore the far-field flow due to an arbitrary solid body is that of a dipole (Batchelor 1967, p. 399). The partial drift volume due to an arbitrary body may be approximated by studying flow around a sphere.

Consider a marked plane S_0 whose perimeter is B_0 in the (y, z)-plane a distance x_0 from the sphere and let R be the radius of the largest circle centred on the x-axis which lies within S_0. The notation is shown in figure 9. The marked plane is distorted by the sphere to give a surface S_t, whose perimeter is B_t. Let S be the projection of S_t onto the (y, z)-plane, i.e. S is also bounded by B_t, but lies entirely in the (y, z)-plane. Also, $\mathscr{V}_t$ is the volume bounded by the surfaces S_t, S_0 and the surface generated as the perimeter B_t is advected along. Let $\mathscr{V}$ be the volume enclosed by the surfaces S, S_0 and the surface traced by B_t.

For flow around a sphere, when the velocity potential is given by (2.1a), the general expression (4.5) becomes

$$X(x_0, y_0, z_0, t) = \frac{1}{U} \left[\frac{A \cos \theta}{r^2} \right]_{(r_0, \theta_0)}^{(r_t, \theta_t)} + \frac{1}{U} \int_0^t q^2 \mathrm{d}t, \tag{4.8}$$

where $A = \frac{1}{2} U a^3$ is the dipole strength of the sphere.

The partial drift volume for the sphere is

$$D_p = \int_S X \mathrm{d}S = \frac{A}{U} \int_S \left[\frac{\cos \theta_t}{r_t^2} - \frac{\cos \theta_0}{r_0^2} \right] \mathrm{d}S + \frac{1}{U} \int_S \int_0^t q^2 \mathrm{d}t \mathrm{d}S. \tag{4.9}$$

By definition, the solid angle subtended by S_0 to the centre of the sphere is

$$\omega_{S_0} = \int_{S_0} \frac{\cos \theta_0}{r_0^2} \mathrm{d}S, \tag{4.10}$$

while the solid angle subtended by S to the centre of the sphere is

$$\omega_S = -\int_S \frac{\cos \alpha}{r^2} \mathrm{d}S. \tag{4.11}$$

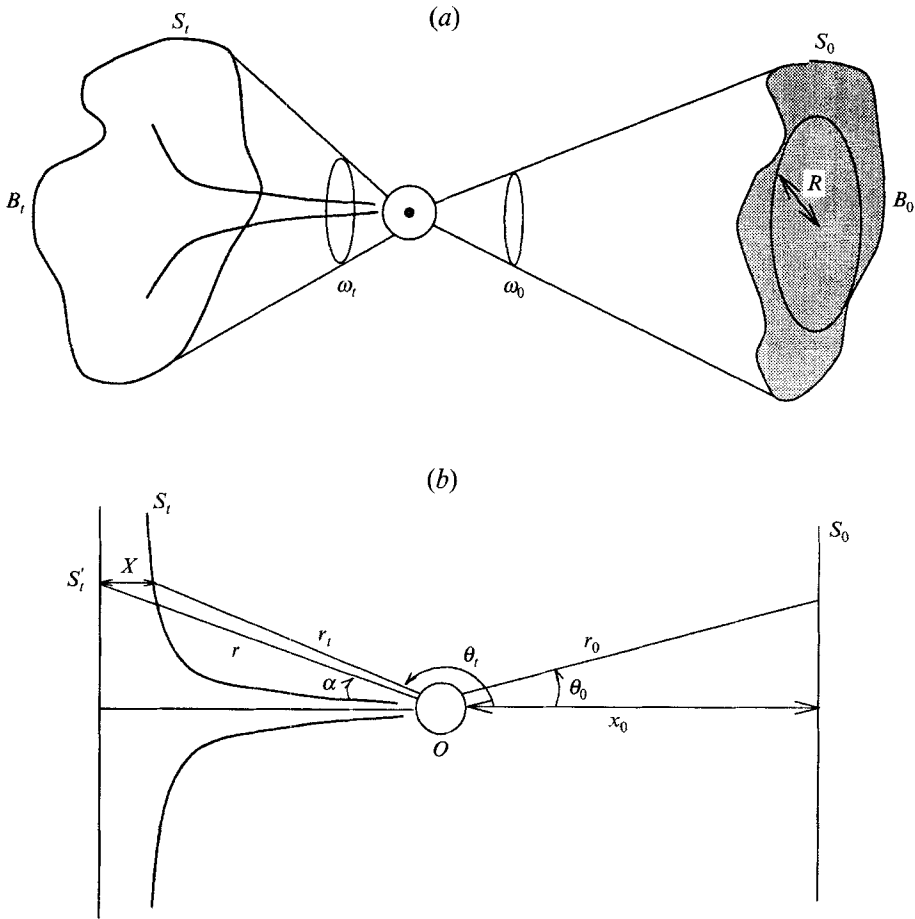When the plane S_0 is much larger than the sphere (i.e. $R \gg a$) and $|x_0 - Ut| \gg a$, it

FIGURE 9. Notation for the distortion of an arbitrary-shaped plane by a sphere.

can be shown that (see Appendix)

$$\int_S \int_0^t q^2 \mathrm{d}t \mathrm{d}S \sim U \int_{\mathscr{V}} \frac{q^2}{U^2} \mathrm{d}\mathscr{V}, \quad \omega_{S_0} \sim \int_S \frac{\cos\theta_0}{r_0^2} \mathrm{d}S, \quad -\omega_S \sim \int_S \frac{\cos\theta_t}{r_t^2} \mathrm{d}S.$$

$$(4.12a, b, c)$$

Substituting the approximations (4.12 a,b,c) into (4.9), we find that the partial drift volume can be written in terms of the solid angles subtended by the marked plane to the centre of the sphere at its initial and final positions:

$$D_p \sim -\frac{A}{U}(\omega_S + \omega_{S_0}) + \int_{\mathscr{V}} \frac{q^2}{U^2} \mathrm{d}\mathscr{V}. \tag{4.13}$$

This equation can interpreted physically. The integrated Lagrangian volume flux through the area with perimeter B_t, i.e. D_p, is equal to two terms. The first is the volume through B_t associated with the momentum of the fluid in $\mathscr{V}$ due to the presence of the body. Theodorsen (1941) derived this first term when calculating the momentum in a sub-region of an unbounded fluid due to the presence of a solid body. The momentum of an unbounded fluid cannot be evaluated using the integral method since the integrals are non-absolutely convergent. The presence of this momentum

term in the expression for partial drift volume means that the partial drift volume is also non-absolutely convergent when $\rho_{max} \to \infty$ and $x_0 \to \infty$. The second term is the volume through B_t associated with the kinetic energy of the fluid in $\mathscr{V}$ due to the presence of the body. The second term is positive and represents a volume of fluid drifting with the body.

When the sphere lies within $\mathscr{V}$ the last term is approximately $C_M V$, the volume of fluid associated with the hydrodynamic mass of the solid body, where C_M is the added-mass coefficient of the sphere and V is its volume. Whereas, if the sphere does not lie within $\mathscr{V}$, then the last term in (4.13) is neglible. Therefore, provided the sphere passes through the marked plane

$$D_p \sim -\frac{A}{U}(\omega_S + \omega_{S_0}) + C_M V. \tag{4.14}$$

This equation is exact when $x_0 \to \infty$, $R \to \infty$ and $t \to \infty$.

We can generalize (4.14) to flow around an arbitrarily shaped three-dimensional solid body. Consider separately the contributions to reflux from outside and inside a circular plane of radius b. Outside this circle, the flow disturbance due to the body is at leading order equivalent to a collection of dipoles of total strength A. The generalization of (4.14) to an arbitrary body then relies on showing that, if the marked plane is sufficiently large and far away, then the contribution to reflux from the circle is small. The partial drift volume is given by

$$D_p \sim -\frac{A}{U}(w_S + w_{S_0}) + O\left(\frac{A}{U}\pi b^2\left(\frac{1}{x_t^2} + \frac{1}{x_0^2}\right)\right) + \int_0^b \left[\frac{\phi}{U} + x\right]_0^t 2\pi y\,dy + C_M V. \tag{4.15}$$

Here the sum of the first two terms is the reflux due to the dipole outside the circle; the third is the reflux inside the circle; and the fourth is the volume drifting with the body. The third term is of

$$O\left(\pi b^2 (\phi/U + x)_{(x_0,0)}^{(x_0-Ut,0)}\right)$$

when $|x_0 - Ut| \gg b$ and $|x_0| \gg b$. In the far field, the velocity potential is that of a dipole so that the third term is

$$O\left(\frac{A}{U}\pi b^2\left(\frac{1}{(x_0 - Ut)^2} + \frac{1}{x_0^2}\right)\right).$$

Therefore, when the plane is much larger than the circle, i.e. $R \gg b$, and the initial and final position of the marked plane is far from the solid body, (4.14) holds.

Similarly, partial drift area for flow around two-dimensional bodies can be expressed as

$$D_p \sim -\frac{A}{U}(\alpha_t + \alpha_0) + C_M V, \tag{4.16}$$

where α_t, α_0 are the angles subtended by the line of marked particles to the centre of the solid body, A the equivalent strength of the dipoles and $C_M V$ area of fluid associated with the hydrodynamic mass of the body.

5. An example of drift in bounded flow

In practical applications the flow is bounded, and the drift is different to unbounded flow. In unbounded flow partial drift volume is single valued and equal to the negative
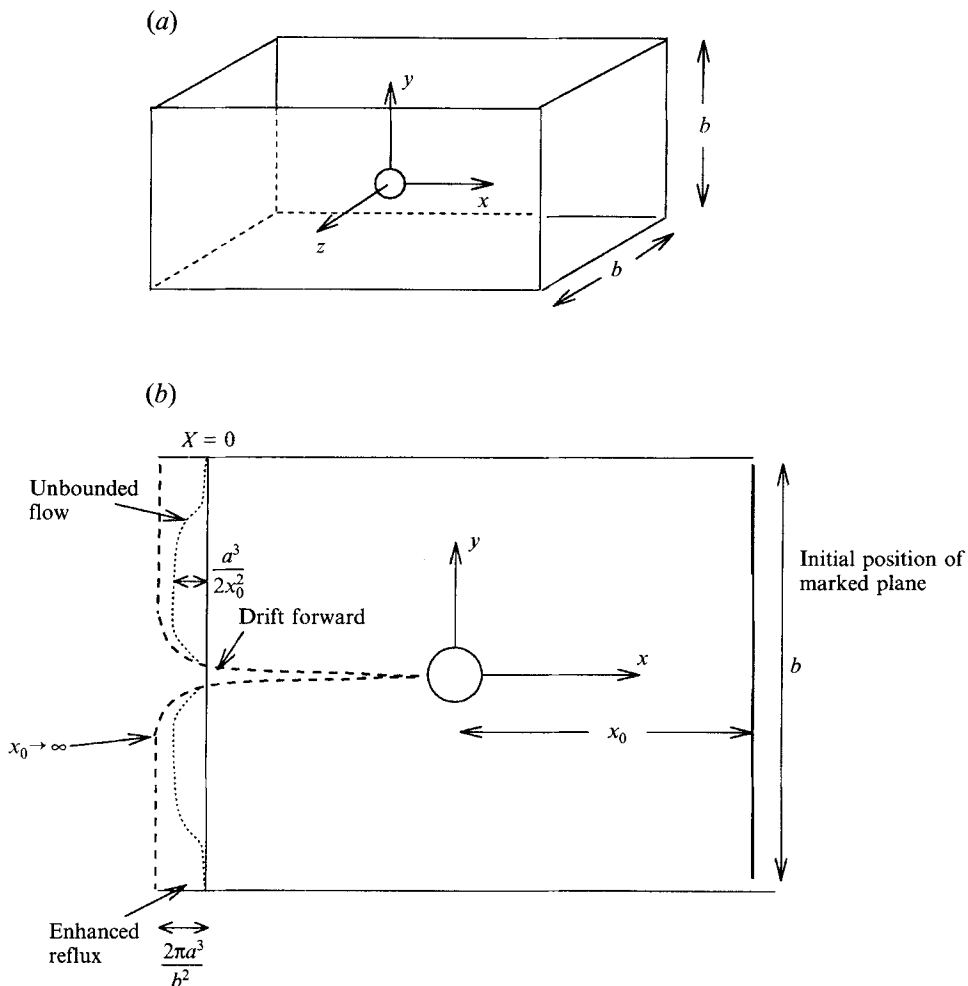
(*a*)

(*b*)

FIGURE 10. An example of partial drift in bounded flow. (*a*) Notation, (*b*) reflux of fluid is shown when $x_0 \rightarrow \infty$. A comparison with unbounded flow is shown.

of the volume of the solid body (Darwin 1953). Darwin 1953 discussed bounded flow, stating that there are two contributions to the partial drift volume: a volume of fluid drifting with the body and a reflux volume which is spread across the cross-section of bounded flow. He illustrated these effects using the two-dimensional example of the drift due to a cylinder moving between two solid planes. We now use our results to discuss the distortion of a marked plane by a sphere travelling along the centreline of a long square tube of side *b*, whose dimensions are much larger than the radius of the sphere, *a*. The notation is shown in figure 10. This example is interesting in light of the experiments of Bataille *et al.* (1991).

The velocity potential for flow around a sphere in unbounded flow is identical to that of a single dipole. The velocity potential for fluid flow around a sphere in a large square tube is calculated by the method of images (Lamb 1932, p. 131), where extra dipoles are introduced so that the kinematic boundary conditions on the solid surfaces are satisfied. When dipoles of strength $\frac{1}{2}a^3 U$ are distributed as shown in figure 11, then the fluid velocity normal to the tube walls is zero. The kinematic
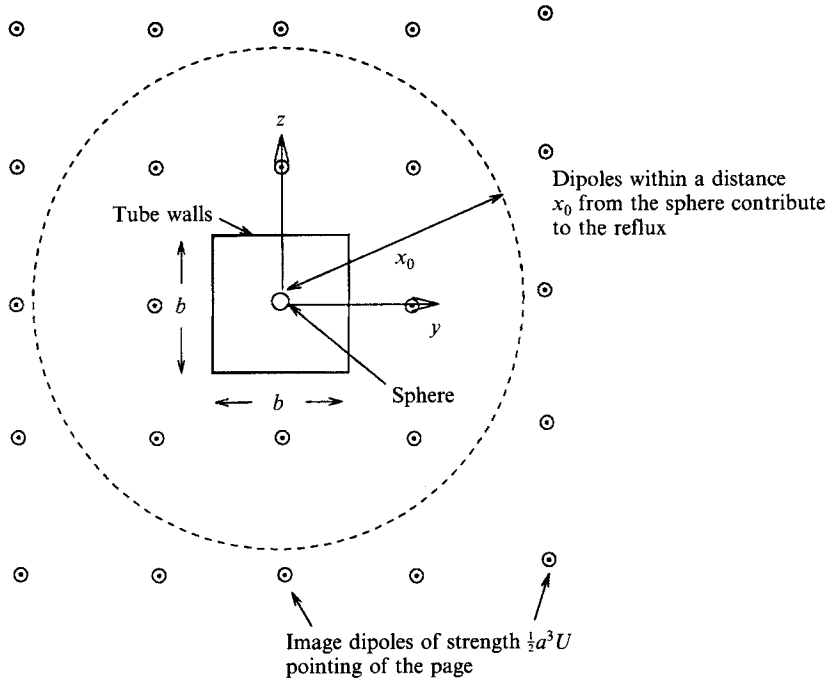
FIGURE 11. The distribution of image dipoles required to satisfy the kinematic condition on the sides of the tube.

boundary condition on the sphere is satisfied by introducing additional dipoles of strength $O(\frac{1}{2}a^3 U a^3/b^3)$, which are neglible when $b \gg a$. The velocity potential is a linear combination of the potentials due to all these dipoles, so that

$$\phi \sim -Ux - \tfrac{1}{2}Ua^3 \left(1 + O(a^3/b^3)\right) \sum_{i,j=-\infty}^{\infty} \frac{x}{(x^2 + (y + ib)^2 + (z + jb)^2)^{3/2}}, \qquad (5.1)$$

where i, j are integers.

The volume of fluid drifting with a sphere in bounded flow is the same as for unbounded flow except for the modificaiton due to image dipoles. The fluid drifting with the sphere is $4\pi A/U - V$ (Taylor 1928), where A is the total dipole strength within the sphere and V the volume of the sphere. Now $A = \frac{1}{2}a^3 U(1 + O(a^3/b^3))$, where the $O(a^3/b^3)$ corrections are from the image dipoles used to satisfy the kinematic boundary condition on the sphere surface. The fluid drifting with the sphere in bounded flow therefore approaches that of unbounded flow when $b \gg a$.

However, the reflux in bounded flow differs substantially from unbounded flow – this can be shown by calculating the negative Lagrangian displacement of a marked plane initially far in front of the sphere. The distribution of reflux across the cross-section of the tube depends on the ratio b/x_0. The negative Lagrangian displacement of a marked fluid element is $[\phi/U + x]_{x_0}^{x_1}$ (from (4.3) and (4.4)). Substituting the velocity potential (5.1), we find that the negative displacement of the particle, X_{neg}, is approximately

$$X_{neg} \sim \tfrac{1}{2}a^3 \sum_{i,j=-\infty}^{\infty} \left[\frac{x}{(x^2 + (y + ib)^2 + (z + jb)^2)^{3/2}} \right]_{x_0}^{x_1}.$$

If $x_1 \rightarrow -\infty$ and $x_0 \gg b$, the negative Lagrangian displacement is

$$X_{neg} \sim -\tfrac{1}{2}a^3 \sum_{i,j=-\infty}^{\infty} \frac{x_0}{(x_0^2 + (y+ib)^2 + (z+jb)^2)^{3/2}} - \frac{a^3\pi}{b^2}$$

$$= -\frac{1}{2}\frac{a^3}{x_0^2} \sum_{i,j=-\infty}^{\infty} \frac{1}{(1 + (\tilde{y} + ib/x_0)^2 + (\tilde{z} + jb/x_0)^2)^{3/2}} - \frac{a^3\pi}{b^2},$$

where $\tilde{y} = y/x_0$ and $\tilde{x} = x/x_0$. The quantity summed over i and j is $O(1)$ for $|i|, |j| \leqslant x_0/b$. There are $O(\pi x_0^2/b^2)$ combinations of i and j for which $|i|, |j| \leqslant x_0/b$, so that

$$X_{neg} \sim -\frac{1}{2}\frac{a^3}{x_0^2} \times O\left(\pi \frac{x_0^2}{b^2}\right) - \frac{a^3\pi}{b^2} \sim -O\left(\frac{a^3}{b^2}\right).$$

As $x_0 \rightarrow \infty$, the negative displacement of a marked particle in bounded flow is therefore independent of x_0 and constant across the tube. Therefore, as $x_0 \rightarrow \infty$ the reflux is spread uniformly across the tube, agreeing with Benjamin (1986). By contrast reflux in unbounded flow is dependent on x_0 and spread uniformly within a distance x_0 from the centreline (figure 4*b*).

The negative Lagrangian displacement of the marked plane can be calculated exactly when $x_0 \rightarrow \infty$. The reflux volume is equal to $D_p - C_M V$, from (4.14). But the drift volume is equal to $-V$, where V is the volume of the sphere, so that the reflux volume is $-(1 + C_M)V = -2\pi a^3$. In the previous paragraph, we showed that when $x_0 \rightarrow \infty$, reflux is spread uniformly across the tube, so that the negative displacement of the marked plane is $-2\pi a^3/b^2$, since the cross-sectional area of the tube is b^2. It is important to note that though the negative displacement $-2\pi a^3/b^2$ is a small quantity, reflux volume, which equals $-2\pi a^3$, is not.

When $a \ll x_0 \ll b$, the reflux of the fluid can be examined qualitatively by studying the contribution to reflux from a single image dipole close to the tube wall. Figure 12 shows the separate contribution to reflux from the image dipole and sphere, and also the combined contribution. We see that the presence of the boundary enhances reflux and that there is a significant variation of reflux within a distance $O(b/2 - x_0)$ of the boundaries.

When $b \sim a$, more (positive) image dipoles are required within the sphere and hence the volume of fluid associated with the hydrodynamic mass, $D = 4\pi A/U - V$ (Taylor 1928), increases. The volume of fluid drifting with the sphere therefore increases. Since the flow is bounded, partial drift volume is constant and the reflux volume decreases, i.e. becomes more negative.

6. Conclusion

We have calculated asymptotic expressions for horizontal Lagrangian displacement, X, of a marked fluid element due to the motion of a sphere. Far from the centreline it was shown that $X < 0$ for certain finite values of x_0, which is in contrast to previous investigations that predicted $X > 0$ for infinite x_0. The partial drift volume was evaluated numerically using a combination of numerical results and asymptotic formulae, and compared with analytical expressions. The partial drift volume was found to be critically dependent on the ratio ρ_{max}/x_0, which explains why Darwin's proposition can only be proved if ρ_{max}/x_0 is specified. In §3 we show how Darwin's proposition may be stated as a mathematical theorem.

Image dipole

Reflux due to image dipole

Reflux due to sphere moving to $x_1 = -\infty$ is $\dfrac{\pi a^3}{b^2}$

Enhanced reflux near boundary

$\dfrac{a^3}{2x_0^2}$

y

Sphere in tube

Initial position of marked plane

b

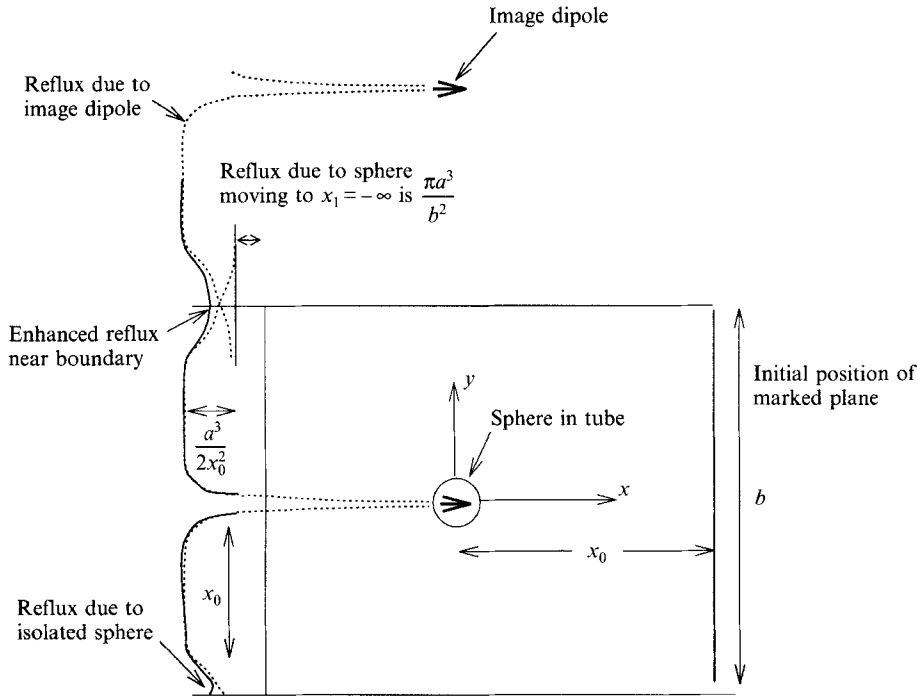x

x_0

Reflux due to isolated sphere

x_0

FIGURE 12. The separate contributions to the reflux from the sphere and nearest image dipole are shown for $a \ll x_0 \ll b$. The total reflux varies significantly close to the tube walls.

A general expression has been derived for the horizontal Lagrangian displacement of a fluid particle due to an arbitrary potential flow superimposed on a constant velocity. The displacement is the sum of two contributions: a drift forward and a reflux backwards. This new expression for Lagrangian displacement was used to calculate the partial drift volume due to a sphere and it was shown that there are two contributions to the partial drift volume. One is the volume associated with the kinetic energy of a region of the fluid and was obtained by Darwin. The second new contribution is the volume associated with the momentum of a region of the fluid, which is proportional to the sum of the solid angles subtended to the centre of the sphere by the marked plane at its initial and final positions. This expression for the partial drift volume could be generalized to arbitrary three-dimensional solid bodies because they have a dipole flow in the far field.

An example of drift due to a sphere in flow bounded by a square tube was given illustrating differences between bounded and unbounded flows. The reflux volume was shown to depend on the initial separation of the marked plane compared with the width of the tube. This example has practical applications.

We are now using the concept of partial drift volume to examine how dust is entrained in the wake of a sand particle as it leaves the ground by calculating the distortion of a plane of marked particles by a sphere moving away from a solid boundary.

are grateful for helpful conversations with Dr G. Duursma and Dr J.R. Ockendon concerning bubbles in bounded flow.

Appendix

To show (4.12a), we first note that the streamfunction, ψ, is related to ρ_0 by $\psi = -\frac{1}{2}\rho_0^2 U$ so that $d\psi = -U\rho_0 d\rho_0$. The streamfunctions for three-dimensional flows are denoted by ψ and χ (Yih 1985). Using (4.2a) we find that

$$dt \, dS = \frac{d\phi}{q^2}(\rho_0 d\rho_0) d\chi = -\frac{d\phi \, d\psi \, d\chi}{U \partial(\phi, \psi, \chi)/\partial(x, y, z)} = -\frac{d\mathscr{V}}{U} \tag{A 1}$$

where $d\mathscr{V}$ is a volume element. Therefore

$$\int_S \int_0^t q^2 dt \, dS = U \int_{\mathscr{V}_t} \frac{q^2}{U^2} d\mathscr{V} = U \int_{\mathscr{V}} \frac{q^2}{U^2} d\mathscr{V} - U \int_{\mathscr{V} \setminus \mathscr{V}_t} \frac{q^2}{U^2} d\mathscr{V}. \tag{A 2}$$

When the sphere has passed far through the marked plane, the second integral is $O(a^9/x'^6)$, whereas if the sphere has not passed through the plane the second integral is $O(a^8/x'^5 \log(a/|x'|))$, where $x' = x_0 - Ut$. In either case, under the assumption of $|x'| \gg a$, the approximation (4.12a) is valid.

To show (4.12b), we transform the area elements on S to the elements on S_0 using (2.3). Thus,

$$y_t dy_t = y_0 dy_0 \left(\frac{1 + \dfrac{3y_0^2 a^3}{2r_0^5}}{1 + \dfrac{3a^3 y_t^2}{2r_t^5}\left(1 + \dfrac{x_t}{y_t}\dfrac{dX}{dy_t}\right)} \right) \tag{A 3}$$

Each position of an area element in the S-plane can be described by cylindrical coordinates (y_t, φ), where φ is the angle the element made the (x, y)-plane. Since there is no rotational drift $dS_t = y_t dy_t d\varphi$ and $dS_0 = y_0 dy_0 d\varphi$. Therefore,

$$\int_S \frac{\cos\theta_0}{r_0^2} dS = \int_{S_0} \frac{\cos\theta_0}{r_0^2} dS_0 + \int_{S_0} \frac{\dfrac{3a^3}{2}\left(\dfrac{\sin^2\theta_0}{r_0^3} - \dfrac{\sin^2\theta_t}{r_t^3} - \dfrac{\sin\theta_t\cos\theta_t}{r_t^3}\dfrac{dX}{dy_t}\right)}{\left(1 + \dfrac{3a^3\sin^2\theta_t}{2r_t^3}\left(1 + \cot\theta_t\dfrac{dX}{dy_t}\right)\right)} dS_0 \tag{A 4}$$

The second term in (A 4) is at most $O(a^2/|x'|, a^2/|x_0|)$ and small when $|x'| \gg a$ and $|x_0| \gg a$, so that approximation (4.12b) is valid.

Equation (4.12c) is derived by using the cosine rule and simple geometrical relations shown in figure 9. We find

$$\int_S \frac{\cos\theta_t}{r_t^2} dS = \int_S \frac{\cos\alpha}{r^2} dS + \int_S \frac{\cos\alpha}{r^3}\left(-r + \frac{r^4}{(r^2 + X^2 - 2rX\cos\alpha)^{3/2}}\right) dS$$
$$- \int_S \frac{X}{(r^2 + X^2 - 2rX\cos\alpha)^{3/2}} dS. \tag{A 5}$$

The second and third integrals are both at most $O(a^3/x_0^2 x')$, so that approximation (4.12c) is valid when $|x'| \gg a$ and $|x_0| \gg a$.

REFERENCES

ABRAMOWITZ, M. & STEGUN, I. A. 1965 *Handbook of Mathematical Functions*. Dover.

BATAILLE, J., LANCE, M. & MARIE, J. L. 1991 Some aspects of the modelling of bubbly flows. In *Phase-Interface Phenomena in Multiphase Flow* (ed. G.F. Hewitt, F. Mayinger & J.R. Riznic), pp. 179–193.

BATCHELOR, G. K. 1967 *An Introduction to Fluid Dynamics*. Cambridge University Press.

BENJAMIN, T. B. 1986 Note on added mass and drift. *J. Fluid Mech.* **169**, 251–256.

DARWIN, C. 1953 Note on hydrodynamics. *Proc. Camb. Phil. Soc.* **49**, 342–354.

KOWE, R., HUNT, J. C. R., HUNT, A., COUET, B. & BRADBURY, L. J. S. 1988 The effects of bubbles on the volume fluxes and the presence of pressure gradients in unsteady and non-uniform flow of liquids. *Intl J. Multiphase Flow* **14**, 587–606.

LAMB, H. 1932 *Hydrodynamics*. Cambridge University Press.

LIGHTHILL, M. J. 1956 Drift. *J. Fluid Mech.* **1**, 31–54 (and Corrigendum **2**, 311–312).

RIVERO, M. 1990 Étude par simulation numérique des forces exercées sur une inculsion sphérique par un écoulement accéléré. PhD thesis, Institute de Mécanique des Fluides de Toulouse, Toulouse.

TAYLOR, G. I. 1928 The energy of a body moving in an infinite fluid, with an application to airships. *Proc. R. Soc. Lond.* A **70**, 13–21.

THEODORSEN, T. 1941 Impulse and momentum in an infinite fluid. *Von Kármán Anniversary Volume*, pp. 49–58. California Institute of Technology.

YIH, C.-S. 1985 New derivations of Darwin's theorem. *J. Fluid Mech.* **152**, 163–172.